Proceedings of the
Annual Stability Conference
Structural Stability Research Council
Atlanta, Georgia, April 21-24, 2020

Study of story drift limits in steel buildings subjected to seismic forces

Andrés F. Robalino[1], Santiago R. Zaruma[2], Telmo A. Sánchez[3]

Abstract
Traditionally, the design of steel buildings for seismic forces initiates by the definition of the lateral force resistant system (LFRS) and the dimensioning of its components for the strength limit states. In addition, construction codes require to limit the inter-story drift to values that commonly range between 1% and 2.5% of the story height. This requirement usually controls the LFRS's design in configurations in which the story lateral rigidity depends on the combination of flexural and axial deformations of the structural components, such as in steel moment frames. In general, drift control is meant to limit the damage in nonstructural components of buildings that could pose a threat to life and to limit lateral displacements and inelastic strains to admissible values, so that the structure remains stable during a seismic event. This paper presents studies conducted to determine the reasonableness of inter-story drift limits specified in different construction codes around the world. Studies are focused on steel moment frames that include the lateral stiffness contribution of nonstructural components, such as division walls and facades. As a result of the study, new criteria for establishing drift limits in steel buildings are proposed, considering the structural integrity of the building and limiting nonstructural damage during a seismic event.

1. Introduction

The history of inter-story drift limits in code provisions shows that depending on the country, there are different approaches to deal with this matter that also change over time. In general, two conditions have been used to check story drift: serviceability and ultimate limit states. In the US, for example, a serviceability drift check was used until 1997 with the intention of minimizing nonstructural damage caused by more frequent minor or moderate earthquakes (SEAOC 2009). This approach was replaced by the ultimate state drift check specified in the 1997 UBC (ICBO 1997), which is intended for severe design earthquake ground motions. This second method was originally developed by ATC 3-06 (ATC 1978), and it requires checking inelastic story drift expected from the design ground motion against a higher drift limit. Since then, the same concept has been used for checking drift in the U.S. and only minor changes have been applied to the specified limits.

[1] Structural Engineer, ADSTREN Cía. Ltda., <arobalino@adstren.com>
[2] Structural Engineer, ADSTREN Cía. Ltda., <szaruma@adstren.com>
[3] President, ADSTREN Cía. Ltda., <tasanchez@adstren.com>

Since ATC 3-06, drift limits as specified in codes from the U.S. have three objectives: limit inelastic deformations in ductile members, limit lateral displacements that may compromise the structural stability of the building, and limit damage in nonstructural components that could pose a life-threatening hazard (ASCE 2016). The allowable story drifts in ASCE 7 are the result of consensus judgements that consider the life-safety and damage control objectives mentioned above. Contrary to common belief, drift limits are not meant to preclude damage in nonstructural components for economic reasons. Extended damage to partition walls, facades, and other nonstructural components, is expected to occur as a result of design-level seismic demands. This is the case even for structures with higher risk categories, since the corresponding drift limits are still higher than damage thresholds for most nonstructural components.

Limiting inter-story drift for strength limit states at the level of the design ground motion is necessary to verify the structural integrity of a building. Inter-story drift, however, is also associated to loss of functionality due to the damage that may occur with seismic events that are of significantly smaller magnitude than the design earthquake. In this context, studies show that most of the economic losses due to earthquakes are associated to the damage to nonstructural components (Taghavi and Miranda 2003). This conclusion is based on the review of the performance of nonstructural components from a database that included more than 4000 records about the damage to components gathered from more than 40 earthquakes. According to this research, there are two reasons for this. First, most of the total construction cost comes from nonstructural components and contents. In a typical commercial building, the structure represents around 20% of the total investment, and the rest is spent on nonstructural components and contents. Fig. 1 shows the cost distribution of three example buildings, including an office building, a hotel and a hospital. Second, damage to nonstructural components is more frequent than damage to structural components. One of the causes for this is that, historically, the focus of building codes has been the performance of structural systems, and nonstructural components have been treated as secondary elements.

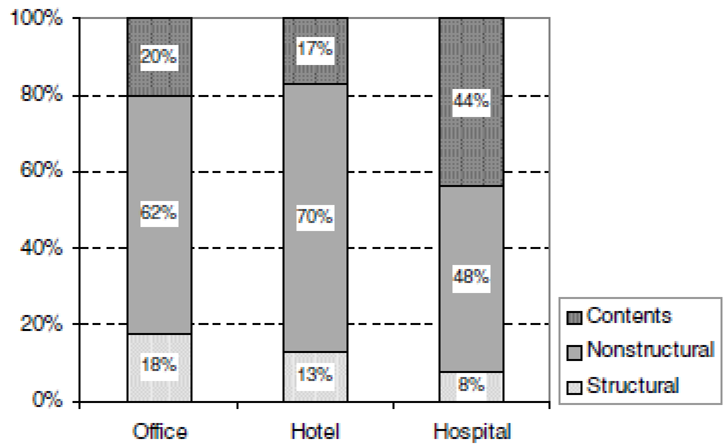

Figure 1: Cost breakdown of office buildings, hotels and hospitals (Taghavi and Miranda 2003)

The issue of controlling damage in nonstructural components is addressed by the ASCE7-16 Standard from two perspectives. The first is establishing limits for story drifts, as described above, and the second is stating specific requirements so that nonstructural components and their connections are designed to accommodate seismic demands without posing a life-threatening hazard. This design philosophy has remained unchanged in this standard for decades. However, as the structural engineering profession moves towards performance-based design, and there are higher expectations of seismic protection, nonstructural components have received more attention and nonstructural damage has been studied in more detail.

The performance-based design approach, which was first established in FEMA 273 and FEMA 274 (ATC/BSSC 1997), is now included in ASCE 41-17 (ASCE 2017). This standard assigns specific acceptance criteria to nonstructural components for different performance levels. For deformation-sensitive components these acceptance criteria are defined in terms of drift limits. For nonstructural masonry in exterior walls, the drift limit is 2% for Life Safety and Position Retention Performance Levels, and 1% for Operational Performance Level. For masonry in partitions (heavy partitions), the drift limit is 1% for Life Safety Level and Position Retention Performance Levels, and 0.5% for Operational Performance Level. The ASCE 41-17 Commentary discusses the use of drift ratio values as acceptance criteria, noting that data on drift ratio values related to damage states are limited, and the use of single median drift ratio values as acceptance criteria must cover a broad range of actual conditions. The values for limiting structural drift ratios were originally derived from the NIBS Loss Estimation Methodology (RMS 1995) and were obtained from experience and very limited test results. Thus, it is suggested that the drift limits for nonstructural components be used as a guide of evaluating the probability of a given damage state for a subject building but not as absolute acceptance criteria. Although ASCE 41 is intended for evaluation and retrofit of existing buildings, it may be used in the design of new buildings.

There have been other initiatives to apply performance-based design in the U.S., such as the TBI Guidelines for Performance-Based Design of Tall Buildings (PEER 2017). These guidelines offer a recommended alternative to the prescriptive procedures of ASCE 7-16 for seismic design of buildings and are intended to result in buildings with similar, and in some cases superior, seismic performance. This document follows a serviceability approach for story drift check, in which calculated story drift shall not exceed 0.5% of story height for a Service-Level Earthquake. While this limit is expected to ensure that permanent lateral displacement of the structure is negligible and to provide some protection to nonstructural components, it is important to recognize that nonstructural damage may not be negligible, particularly in elements like partitions.

Further review of design codes from Canada, Mexico, Colombia, Ecuador, Chile, and New Zealand shows that, in general, most of them follow a similar approach to the one established in ASCE 7-16, i.e., defining a limit for story drift checks at ultimate limit state only. This is the case for the codes from Canada, Colombia, and Ecuador. In addition to the strength check, the codes from Mexico and New Zealand also include a serviceability drift check, based on a ground motion with a smaller return period than the used for strength purposes. In the case of Chile, the design code requires a serviceability drift check only. As previously explained, the objective of a serviceability drift check is to minimize structural and nonstructural damage caused by more frequent minor or moderate earthquakes that would prevent the structure from being used as originally intended or that would cause significant economic losses.

In the case of Ecuador, the seismic design criteria in the applicable code, NEC-SE-DS (MIDUVI 2015), establishes requirements for checking drift limits at ultimate limit states, but there are no specific requirements for drift limits as applied to damage control of nonstructural components. NEC presents a description of the expected performance of nonstructural elements at different hazard levels; nevertheless, it does not provide any guidance on how to achieve such performance or any prescriptive design procedure. This is of particular concern given the characteristics of most of nonstructural components used in the region which are susceptible to significant damage even upon the occurrence of a moderate seismic event.

In Ecuador, the most common type of system used for cladding and partitions is unreinforced masonry (URM) composed by concrete blocks with hollow cores. This type of system is known to be considerably brittle under seismic loading, and this was recently demonstrated by the extended damage observed after the Muisne Earthquake in 2016 (Fig. 2 shows an example).

Figure 2: Cladding damage in a building after the 2016 Muisne Earthquake

As nonstructural components receive more attention, projects to help understand and prevent nonstructural damage have been promoted. The FEMA E-74 Guide (FEMA 2012a) explains the sources of nonstructural earthquake damage and describes methods for reducing potential risks. For the case of cladding and partitions the damage has three main causes: inertial forces, building deformations and separation/pounding between separate structures. The last two causes of damage are related to inter-story drift. ASCE 41-17 classifies nonstructural components in three groups based on their response sensitivity on each primary orthogonal direction as follows: acceleration-sensitive components are sensitive to inertial forces, deformation-sensitive components are sensitive to drift or deformation of the structure, lastly acceleration and deformation sensitive components are sensitive to both elements. The kind of URM commonly used in Ecuador is considered both an acceleration and deformation sensitive component. There are numerous factors affecting the extent to which nonstructural elements are damaged; however, surveys show that exterior finishes, interior finishes and partitions always represent the main portion of damage among nonstructural components (Taghavi and Miranda 2003).

As illustrated above, in the event of an earthquake, the largest loss costs in most buildings is associated to nonstructural components and contents damage. FEMA E-74 divides the potential consequences of nonstructural damage into three types of risk: life safety (LS), property loss (PL), and functional loss (FL). The first type of risk is related to injuries and fatalities that could occur when heavy exterior cladding and partitions fall. In addition, if the damaged element is blocking safe exits in a building, life can also be compromised. Property loss can be the result of direct damage to the nonstructural elements or of the consequences generated by its damage. If a partition falls over the contents of a building, then the overall property loss includes the repair cost of the partition and the cost of the damaged contents, which can be much larger in facilities that store valuable contents, like high tech equipment, art or relics. Finally, nonstructural damage can compromise or completely preclude the normal function of the building. This is usually the most important risk after life safety, because of the economic loss associated to interruptions during restoration which can be larger than the cost of repairing the damage or of replacing the contents. Lastly, even more important than loss of profits, is the suspension of emergency operations of essential facilities, such as hospitals and fire and police stations, which must remain functional after an earthquake. For the typical practice in Ecuador, where mechanical, electrical, and plumbing (MEP) components are inserted within the unreinforced masonry partitions, loss of functionality is very likely to happen after cladding and walls sustain damage during an earthquake.

Although URM walls are nonstructural components, evidence shows that they are engaged with the rest of the structure during a seismic event; especially, when the LFRS is a moment frame. Structural frames with masonry infill walls are prevalent for buildings in the country and these infills are generally ignored in analysis and design. Their influence on the behavior of the structure, however, is significant. Infills can drastically change the global lateral stiffness, increasing the inertial forces that the building experiences, at least during the first part of the earthquake; moreover, their presence can attract forces to parts of the structure that were not designed accordingly. Predicting the seismic response of infilled frames is a difficult task due to its complexity and nonlinearity; nevertheless, typical damage/failure mechanisms have been identified in previous research (Bose et al. 2019). Usually, the failure of URM infill walls under lateral load begins with the detachment of the infill and the frame, which is then followed by shear-friction cracks, diagonal tension cracks, crushing of the corners, or combinations of these. Fig. 3 provides an illustration of this process. These mechanisms describe the in-plane behavior of the infills, and its occurrence weakens the arching action that initially resist out-of-plane loads, which can result in out-of-plane collapse. Fig. 2 shows some of the in-plane failure mechanisms and an out-of-plane collapse.

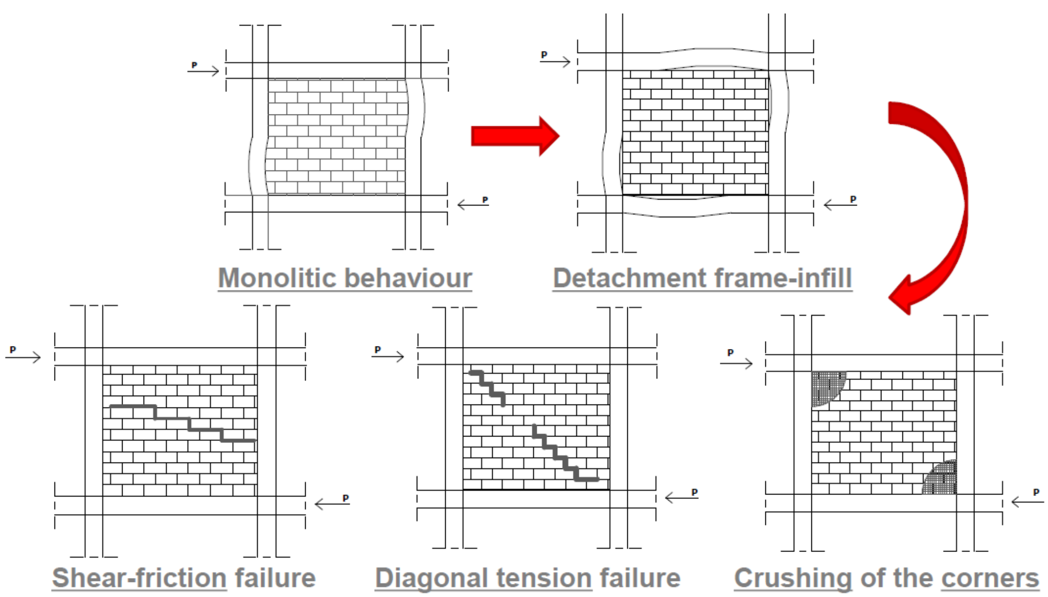

Figure 3: Damage/failure mechanisms for URM infill walls (Rodrigues 2014)

The level of drift at which URM infill walls reach the different damage mechanisms is not precisely known and can vary depending on several factors. Nevertheless, several tests results and data from different standards show consistency about the range at which URM infills reach their peak strength. In a study that tested traditional URM infills (Sahin 2014), for example, a diagonal crack from corner to corner formed at 0.2% drift in one direction, and at 0.3% drift in the other direction, indicating that peak strength was reached. ASCE 41-17 provide a method to determine the drift at peak strength for infilled frame bays according to the ductility of the frame (nonductile or ductile) and the stiffness of the infill (relatively flexible or relatively stiff). For the studies documented in this paper, special steel moment frames (ductile) with URM infill walls (relatively stiff), the drift at peak strength varies within a range starting from 0.15%. Finally, from the collection of fragility data from FEMA P58 (FEMA 2012b), for the case ordinary reinforced masonry walls with partially grouted cells, the median story drift ratio for the first occurrence of major diagonal cracks is 0.2%. This is illustrated in Fig. 4, which shows fragility curves for two damage states of masonry walls; damage state 1 (DS1) corresponds to the first occurrence of major diagonal cracks.

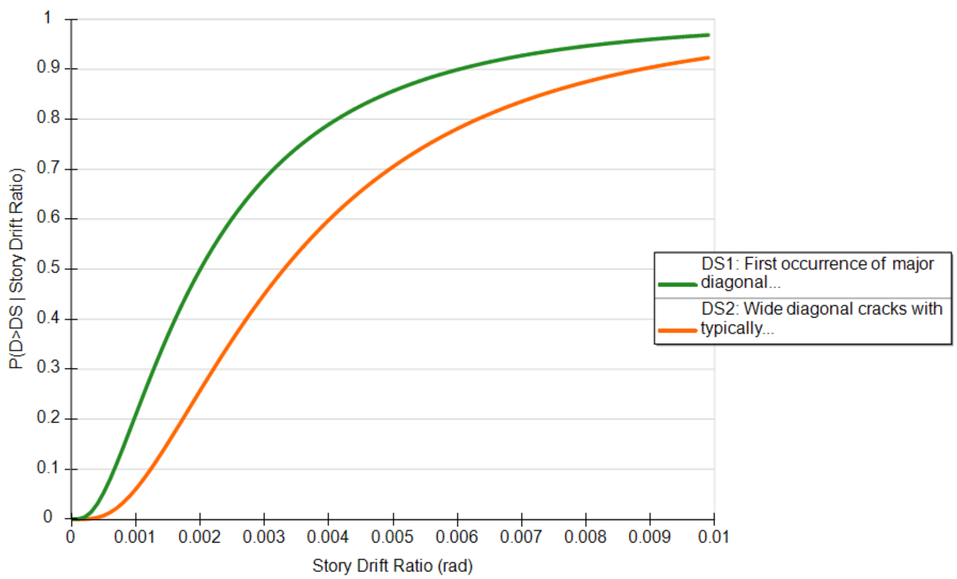

Figure 4: Fragility curves for ordinary reinforced masonry walls with partially grouted cells, shear dominated, 4” to 12” thick, up to 12-foot-tall (FEMA 2012)

Whether or not to reduce current story drift limits to control nonstructural damage has been a recurrent topic of discussion within the structural engineering community in Ecuador. Reducing current drift limits to minimize damage and the cost of building repair due to the occurrence of a seismic event, however, is not effective. Nonstructural damage in facades and partitions occur when the inter-story drift is significantly lower than traditional limits (i.e., 1% to 2.5%). From the data of FEMA P58 (Fig. 4), for example, more than 90% of shear dominated reinforced masonry walls are expected to show serious damage at 1% drift ratio. Hence, it becomes clear that simply reducing the current drift limits is not a solution to the problem since damage occurs at drift limits as low as 0.2%. Therefore, it is more adequate to develop a rational approach that addresses nonstructural damage that includes all of the different factors previously discussed, in addition to limiting the inter-story drift to low levels. A combination of an appropriate methodology to evaluate the structural performance of a LRFS with MCU walls and the implementation of FEMA

E-74 recommendations should result in an improved performance during seismic events of smaller magnitudes than the design earthquake.

Based on the previous discussion, this paper presents the implementation of a serviceability drift check to minimize nonstructural damage in cladding and partitions constructed with unreinforced masonry (URM). Numerical studies were performed for steel special moment resisting frames (SMRF) with unreinforced masonry (URM) infill walls, which consist of concrete blocks with hollow cores. The lateral stiffness contribution of the infill walls was included in the numerical models, according to the properties of typical URM walls constructed in Ecuador. The model, however, could be easily adapted for other regions. The methodology and the resulting new criteria for drift control are presented in the following sections.

2. Numerical Model Description

2.1 Prototype Buildings

The prototype buildings used for this research are based on a one-story structure with plan view and SMRF elevation as shown in Fig. 5. From this baseline configuration three variables are used to define the parametric study: story height (H), bay width (L), and number of frames (N). Three alternatives are chosen for each variable, resulting in a total of 27 models, as listed in Table 1. The SRMF's are assumed to be infilled by URM walls constructed with standard hollow concrete blocks with a nominal thickness of 15cm, which have an effective thickness of 14cm.

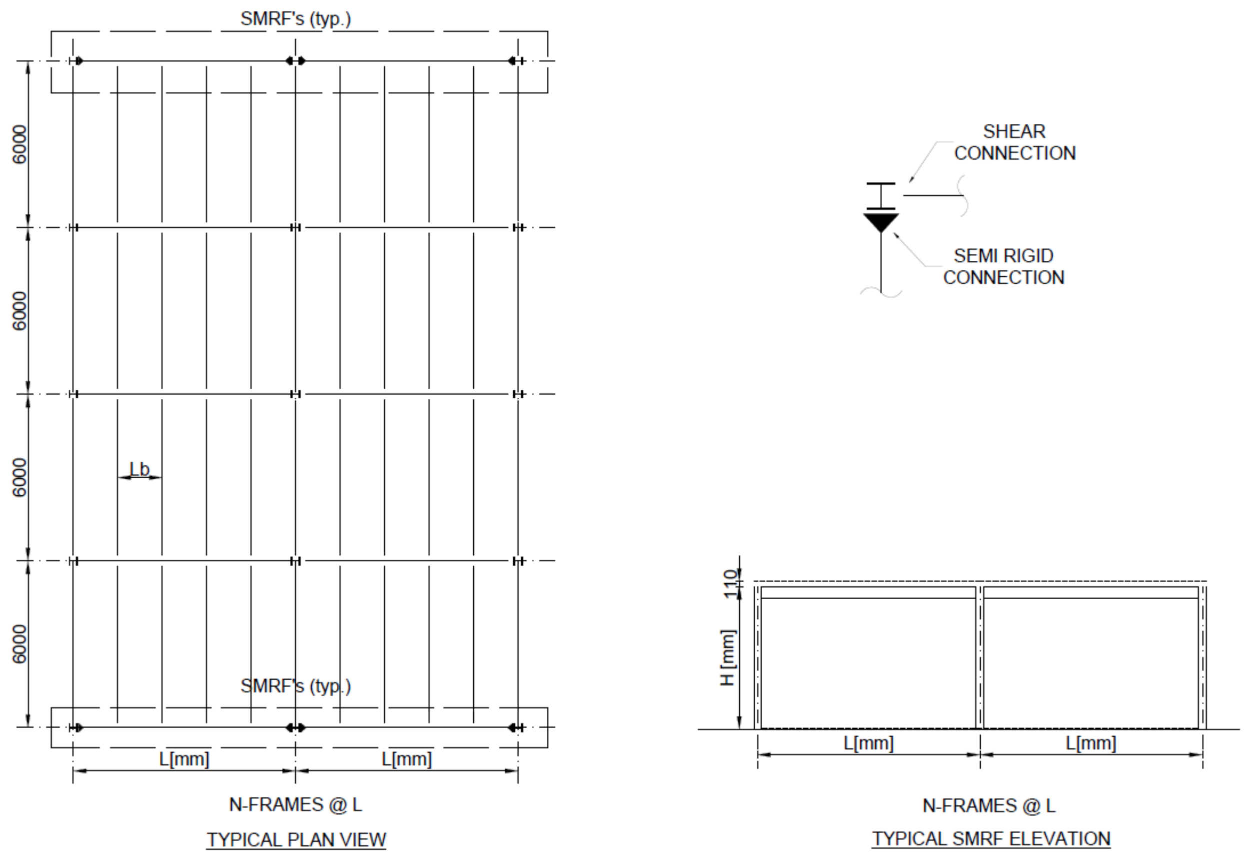

Figure 5: Baseline prototype building

Table 1: Prototype building definition

Prototype building	H (mm)	L (mm)	N
M1	3000	6000	2
M2	4500	6000	2
M3	3750	6000	2
M4	3000	7000	2
M5	4500	7000	2
M6	3750	7000	2
M7	3000	5000	2
M8	4500	5000	2
M9	3750	5000	2
M10	3000	6000	3
M11	3000	6000	4
M12	4500	6000	3
M13	4500	6000	4
M14	3750	6000	3
M15	3750	6000	4
M16	3000	7000	3
M17	3000	7000	4
M18	4500	7000	3
M19	4500	7000	4
M20	3750	7000	3
M21	3750	7000	4
M22	3000	5000	3
M23	3000	5000	4
M24	4500	5000	3
M25	4500	5000	4
M26	3750	5000	3
M27	3750	5000	4

2.2 Seismic Design

The prototype buildings are located in Latacunga, Ecuador, which is a high seismic hazard zone. As previously mentioned, the LFRS considered for these prototypes consists of steel SMRFs. The seismic design is conducted according to the equivalent lateral force procedure from NEC-SE-DS. The steel beams and columns were sized following AISC 360-16 (AISC 2016a) and AISC 341-16 (AISC 2016b), using American wide-flange sections. In NEC-SE-DS, the design base shear, V, is given Eq.1:

$$V=\frac{IS_a(T_a)}{R\varnothing_P\varnothing_E}\ W \tag{1}$$

where $S_a(T_a)$ is the spectral acceleration for the given period of the structure (T_a), $\varnothing_P$ and $\varnothing_E$ are coefficients for irregularity in plant and elevation, I is the importance coefficient, R is the seismic resistance reduction factor, and W is the reactive seismic weight. For this case, $S_a(T_a) = 1.19$, $\varnothing_P$ and $\varnothing_E$ are 1.0, $I = 1.0$, $R = 8$, and W varies depending on the protype building. $S_a(T_a)$ is obtained from the design response spectrum that is constructed as shown in Fig. 6; where, η is a factor normalized as η =2.48 for the region under consideration; r is a factor that depends on the type of soil; F_a is the short-period site coefficient; F_d and F_s is also site coefficients; and z is the peak ground acceleration (PGA). For this case, $r = 1.0$, for the assumed type D soil F_a =1.2, $F_d = 1.19$, $F_s = 1.28$, and $z = 0.40$g. All prototypes fall under the short-period plateau defined by $S_a(T_a) = \eta z F_a$ = 1.19g; $\eta z F_a$ is the equivalent of S_{DS} in ASCE 7-16.

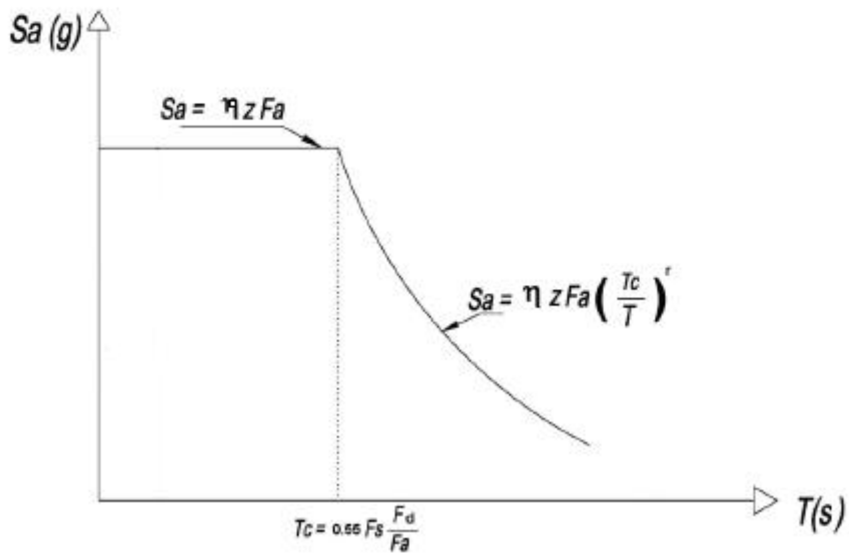

Figure 6: Design response spectrum in NEC-SE-DS

As it is usually the case for SMRFs, the design was controlled by drift limitations. Similarly to the provisions from the United States, the drift limit for this case is 0.02 of the story height, *H.* The calculation of drift in NEC-SE-DS is different, however. Maximum inelastic drift (Δ_M) is calculated as $\Delta_M = 0.75R\Delta_E$, where Δ_E is the elastic drift obtained from the analysis by the application of the design seismic forces. The designed SMRFs were optimized as much as possible to comply with drift limitations; nevertheless, the limiting width-to-thickness ratios for highly ductile members from ASCI 341-16 determined the size of members in several cases.

2.3 Numerical Model

Numerical models in 2D were developed in SAP2000 (CSI 2020) for all design prototypes. Elastic beam elements were used for beams and columns, and a rigid diaphragm condition was applied. URM infill walls were modeled as equivalent diagonal struts, which is a commonly used representation for these components. The equivalent struts have the thickness of the wall and the material properties of the infill, whereas the effective width can be estimated with different empirical equations. For this study, the simple approach of defining the width as on third of the length of the strut was followed (Holmes 1961). The material properties for the equivalent strut were defined based on the results of a study that determined the elastic modulus of unreinforced concrete block masonry as used in Ecuador (Lopez & Ushiña 2017). For this study, 41 masonry prisms were constructed and tested under compression. The obtained stress-strain curves were processed to find an expected elastic modulus of E_m = 388.2MPa. By considering a compressive strength of f'_m = 1.63 MPa, the expected modulus of elasticity is $E_m = 237\ f'_m$. This value is relatively low as compared to relationships obtained from other research, but it is considered appropriate for the type of masonry that was tested and the modeling considerations. The struts are modeled as pinned elements with zero weight. The effective thickness of the block (14cm) was assigned as the thickness of the struts. While a more rigorous modeling of equivalent struts would require them to be compression-only elements, for the purpose of this paper they were modeled as typical axial elements. Due to the configuration of the models and the type of numerical testing used for this research, tension load in struts is negligible. Furthermore, the use of compression-only elements would require nonlinear analysis. To confirm that use of these conditions produced no significant difference in the results, a nonlinear analysis with compression only elements was performed, nevertheless.

3. Study framework

3.1 Performance objective

According to NEC-SE-DS philosophy, nonstructural elements shall present no damage under a service-level seismic hazard, which is defined as an earthquake having a 43-year mean recurrence interval. As previously mentioned, however, the code does not provide any guidance on how to achieve such performance. Regarding the objective of this paper, the first issue that arises is to define a level of drift at which damage in URM infill walls is non-existent. URM infills are considered to show no damage until they reach their peak strength and then present a brittle failure. The tests results and data from ASCE 41-17 and FEMA P58, described above, were contemplated to define 0.2% as the drift limit up to which URM infill walls present negligible damage. The second issue is to check the reasonableness of the service-level earthquake definition, a task that was also addressed with the analyses completed for this paper.

3.2 Analyses

Linear static analyses were performed for all prototypes with the inertial force distribution as it was applied for design. The procedure for each prototype consisted in applying lateral force until a 0.2% drift was reached and recording the value of this force. Table 2 shows the results of this process, where the base shear at 0.2% is recorded as a fraction of $S_a(T_a)$. The base shear percentage resisted by columns and struts is also reported for reference, and the mean value for each variable is included, as well. Results show that the struts receive most of the load, with a mean of 83% of the total base shear. The values of base shear at 0.2% drift are fairly close to each other, and the mean is $0.46S_a(T_a)$ = 0.46 (1.19g) = 0.55g. The next step is to determine the recurrence interval (or return period) associated to the base shear obtained in the analyses.

NEC-SE-DS provides seismic hazard curves that relate the peak ground acceleration with the annual exceedance probability (AEP) for each region in Ecuador. For example, the seismic hazard curve for Latacunga is shown in Fig. 7. Recalling that the plateau of the spectrum is given by $S_a(T_a) = \eta z F_a$, for a plateau value of 0.55g, the value of z (peak ground acceleration) is given by z = 0.55g/(ηF_a) = 0.18g. From Fig. 7, for a PGA of 0.18g, the approximate annual exceedance probability is 0.02. Finally, the recurrence interval is the inverse of the AEP, resulting in a 50-year recurrence interval. This value is close to the 43-year recurrence interval considered as service-level earthquake in NEC-SE-DS and appears to be appropriate for a serviceability drift check.

Table 2: Analyses results

Prototype building	Percentage of base shear at columns (%)	Percentage of base shear at struts (%)	Base shear at 0.2% drift (fraction of $S_a(T_a)$)
M1	17%	83%	0.44
M2	16%	84%	0.51
M3	16%	84%	0.49
M4	19%	81%	0.41
M5	17%	83%	0.49
M6	19%	81%	0.46
M7	17%	83%	0.48
M8	16%	84%	0.51
M9	16%	84%	0.50
M10	18%	82%	0.42
M11	21%	79%	0.43
M12	15%	85%	0.49
M13	17%	83%	0.48
M14	16%	84%	0.46
M15	16%	84%	0.44
M16	19%	81%	0.38
M17	19%	81%	0.37
M18	17%	83%	0.47
M19	16%	84%	0.46
M20	18%	82%	0.44
M21	18%	82%	0.43
M22	17%	83%	0.46
M23	16%	84%	0.45
M24	16%	84%	0.50
M25	16%	84%	0.50
M26	15%	85%	0.49
M27	16%	84%	0.48
Mean	17.0%	83.0%	0.46

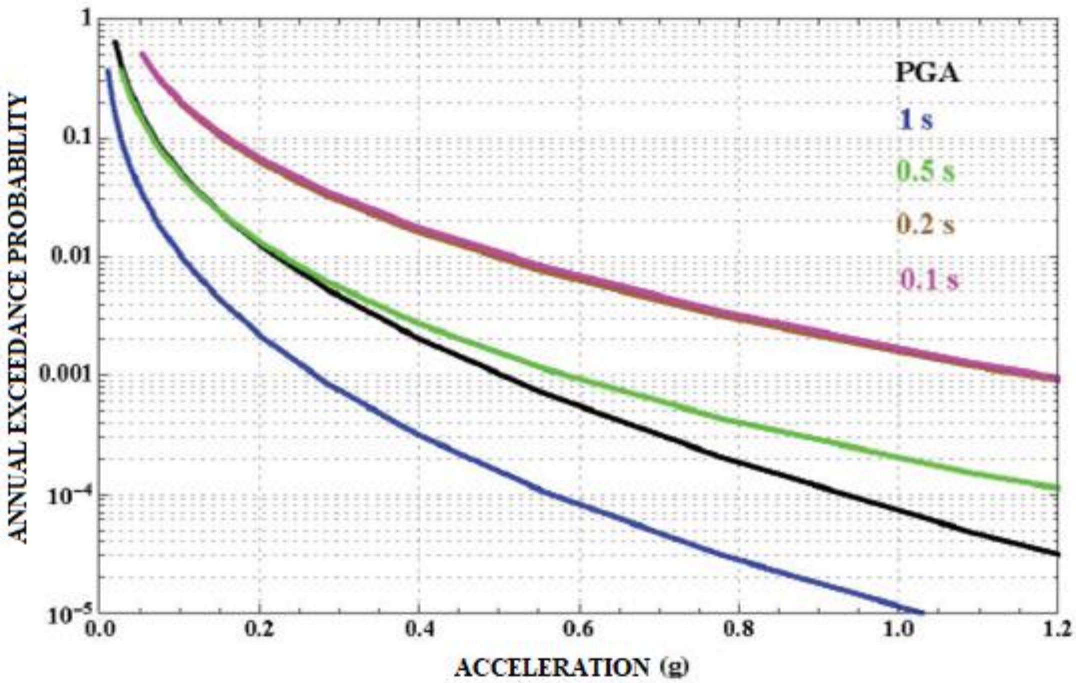

Figure 7: Seismic Hazard Curve for Latacunga

The influence of the frame dimensions is presented next. As previously stated, three parameters are varied in the study: the floor height, *H*, the floor width, *W*, and the number of bays, *N*. Fig. 8 shows that as the story height increases the base shear associated to the 0.2% drift also increases. Fig. 9 shows that as the bay width increases the base shear decreases. Finally, Fig. 10 shows that with an increment of the number of bays, the base shear increases.

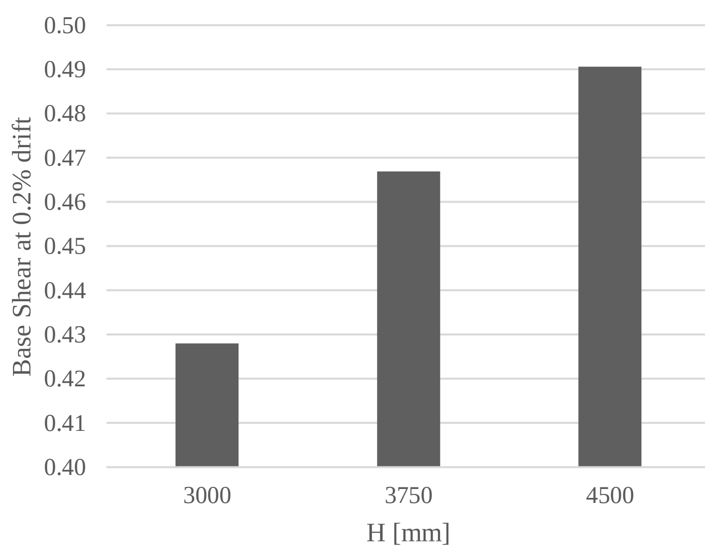

Figure 8: Mean base shear at 0.2% drift vs. story height (H)

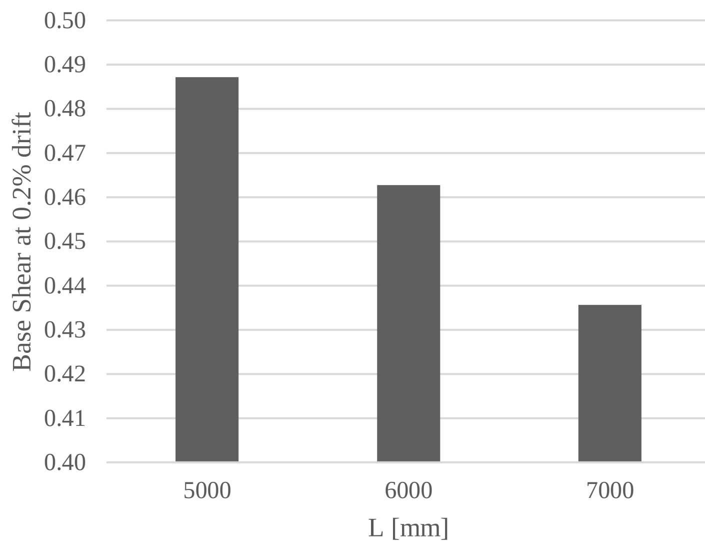

Figure 9: Mean base shear at 0.2% drift vs. bay width (L)

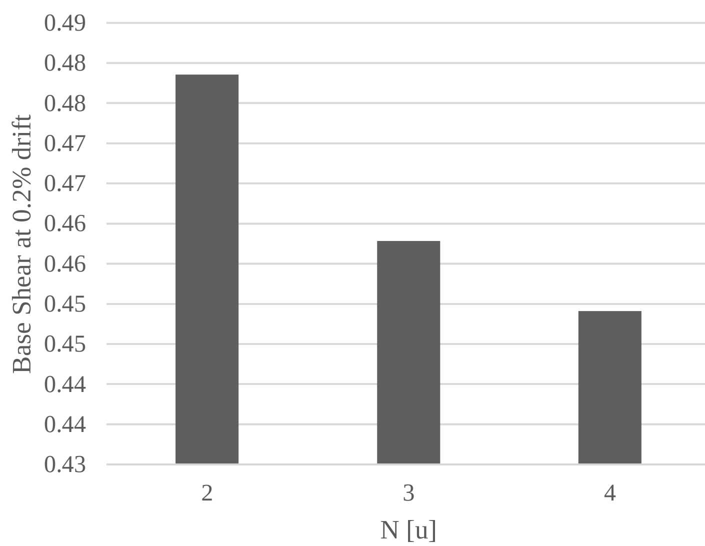

Figure 10: Mean base shear at 0.2% drift vs. number of frames (N)

4. Proposed criteria for damage control

Based on the results presented in the previous section, the following procedure is proposed to conduct analyses for damage control in buildings with moment frames and MCU walls. Essentially, these criteria result in a drift check at serviceability limit sate, which is composed by the following steps.

4.1 Step 1: Modeling the structure with URM infill walls

A numerical model that includes the lateral stiffness contribution URM infill walls is needed for analysis. While numerous models for URM infill walls have been proposed by researchers, a simplified model is considered appropriate for the purpose of these criteria. This simplified model consists of an equivalent diagonal strut with a thickness corresponding to the effective thickness of the blocks and a width of one third of the strut. The material properties of the strut should be obtained from testing, preferably. For the case of URM constructed in Ecuador, a compressive strength of f'_m = 1.63 MPa and an elastic modulus of E_m = 388.2 MPa can be used. These values were obtained from the experimental testing described above.

4.2 Step 2: Apply a service-level earthquake load

While a service-level earthquake is already defined in NEC-SE-DS and other standards, a ground motion with a 50-year recurrence interval is proposed as the service-level earthquake for these criteria. The force applied to the structure should correspond to the short-period plateau of a response spectrum defined with this recurrence interval. Until the walls crack, structures with URM infill walls are considerably rigid structures and their fundamental period will be under the limit for the short-period plateau. Hence, for NEC-SE-DS the service-level seismic load is given by $\eta z F_{a,}$, where z is the peak ground acceleration corresponding to a 50-year recurrence interval, or 0.02 annual exceedance probability. This load is applied through an elastic analysis.

4.3 Step 3: Verify that the elastic drift under service-level earthquake does not exceed 0.02%

As explained above, based on tests results and data from standards, 0.2% was defined as the drift limit up to which URM infill walls present no damage, being this the performance objective under a service-level demand. Since the applied load corresponds directly to the response spectrum, the calculated drift from the elastic analysis (elastic drift) does not need to be amplified.

5. Conclusions

This paper presents a review of the knowledge and criteria regarding story drift limitations and its relationship with nonstructural damage; furthermore, new criteria is proposed for drift control to minimize damage in cladding and partitions constructed with unreinforced masonry (URM), a particularly common practice in Ecuador.

The methodology proposed in this paper consists of a serviceability drift check. This approach of drift control has been used in codes from different countries and it presents an alternative that poses more attention to nonstructural components. While URM infill walls are typically ignored during analysis and design, they are considerably influential in the behavior of the structure. Thus, including these elements in numerical models was recognized as the first piece to be incorporated in new criteria. A simple method of modeling these elements was found in literature and is recommend in this study. A recurrence interval to define a service-level earthquake is also suggested based on the results from numerical analyses. Finally, a maximum allowable story drift of 0.2% is advised for the verification at service limit state, based on literature review.

6. Future work

The discussion from previous sections shows that further studies are required to better address the issue of controlling drift with the purpose of minimizing damage in nonstructural components. The numerical analyses performed for this research are limited and there are many other variables affecting the behavior of URM infill walls that need to be explored. Further numerical and experimental testing is needed to refine the proposed criteria. The global behavior of SMRF with URM infill walls need to be calibrated with results from laboratory testing. Lastly, the definition of both a service-level earthquake and a drift limit corresponding to this level of demand probably need to be adjusted after more studies are performed. The authors will conduct further research on these topics and results will be presented in future papers.

References

Structural Engineers Association of California (SEAOC). (2009). *SEAOC Blue Book: Seismic Design Recommendations*, Sacramento, CA.

International Conference of Building Officials (ICBO). (1997). *Uniform Building Code*, Whittier, CA.

Applied Technology Council (ATC). (1978). *Tentative Provisions for the Development of Seismic Regulations for Buildings (ATC 3-06)*, Washington, D.C.

American Society of Civil Engineers (ASCE). (2004). *Minimum design loads for buildings and other structures. ASCE/SEI 7-16.* Reston, VA: American Society of Civil Engineers/Structural Engineering Institute.

Taghavi, S., & Miranda, E. (2003). *Response Assessment of Nonstructural Building Elements.* Berkeley: Pacific Earthquake Engineering Research Center.

ATC/BSSC. (1997). *NEHRP Guidelines for the Seismic Rehabilitation of Buildings FEMA 273*, prepared by the Applied Technology Council for the Building Seismic Safety Council, published by the Federal Emergency Management Agency, Washington, D.C.

ATC/BSSC. (1997). *NEHRP Commentary on the Guidelines for the Seismic Rehabilitation of Buildings FEMA 274*, prepared by the Applied Technology Council for the Building Seismic Safety Council, published by the Federal Emergency Management Agency, Washington, D.C.

Risk Management Solutions Inc (RMS). (1995). *Development of a Standardized Earthquake Loss Estimation Methodology. Volume 1*. Prepared by Risk Management Solutions Inc., for the National Institute of Building Sciences, Washington, D.C.

Pacific Earthquake Engineering Research Center (PEER). (2017). *Guidelines for Performance-Based Seismic Design of Tall Buildings.* Developed by the Pacific Earthquake Engineering Research Center as part of the Tall Buildings Initiative, Berkeley, CA.

Ministerio de Desarrollo Humano y Vivienda (MIDUVI). (2015*). Norma Ecuatoriana de la Construcción: Peligro Sísmico, Diseño Sismo-resistente, NEC-SE-DS.*

FEMA. (2012a). *Reducing the Risks of Nonstructural Earthquake Damage* - A Practical Guide *FEMA E-74*, Federal Emergency Management Agency, Washington, D.C.

Bose, S., Martin, J., & Stavridis, A. (2019). "Simulation Framework for Infilled RC Frames Subjected to Seismic Loads." *Earthquake Spectra,* 35(4) 1729-1762., Federal Emergency Management Agency, Washington, D.C.

Rodrigues, H. (2014, Jul.). "Numerical Modeling of masonry infill walls participation in the seismic behavior of RC buildings." *Workshop on Multi-Hazard Analysis of Structures using OpenSees – OpenSeesDays.* Porto, Portugal.

FEMA. (2012b). *Seismic Performance Assessment of Buildings FEMA P-58,* prepared by the Applied Technology Council for the Federal Emergency Management Agency, Washington, D.C.

AISC. (2016a). *Specification for Structural Steel Buildings ANSI/AISC 360-16*. American Institute of Steel Construction. Chicago, IL.

AISC. (2016b). *Seismic Provisions for Structural Steel Buildings ANSI/AISC 341-16*. American Institute of Steel Construction. Chicago, IL.

CSI. (2020). *SAP2000 Integrated Software for Structural Analysis and Design*. Computers and Structures Inc., Berkeley, CA.

Holmes, M. (1961). *Steel frames with brick work and concrete filling*. ICE Proceedings.